

AD-A100 732

NAVAL OCEAN SYSTEMS CENTER SAN DIEGO CA  
A HIGH PERFORMANCE FIBER OPTIC PRESSURE PENETRATOR FOR USE IN TH---ETC(U)  
FEB 81 S J COWEN  
NOSC/TR-644

F/G 20/6

UNCLASSIFIED

NL

1 of 1  
AD A  
0100732

NOSC

9

END  
DATE  
7-81  
DTIC

KJ  
E

II

(12)

# NOSC

NOSC TR 644

NOSC TR 644

## Technical Report 644

### A HIGH-PERFORMANCE FIBER OPTIC PRESSURE PENETRATOR FOR USE IN THE DEEP OCEAN

SJ Cowen

26 February 1981

Progress Report: January 1980—January 1981

Prepared for  
NOSC Independent Exploratory Development Program  
Naval Air Systems Command, Fiber Optic Block Program

Approved for public release; distribution unlimited.

---

NAVAL OCEAN SYSTEMS CENTER  
SAN DIEGO, CALIFORNIA 92152

1010 FILE COPY



NAVAL OCEAN SYSTEMS CENTER, SAN DIEGO, CA 92152

---

A N A C T I V I T Y O F T H E N A V A L M A T E R I A L C O M M A N D

---

**SL GUILLE, CAPT, USN**

*Commander*

**HL BLOOD**

*Technical Director*

**ADMINISTRATIVE INFORMATION**

This work was sponsored in FY 80 by Code 013 of the Naval Ocean Systems Center, San Diego, CA, as an Independent Exploratory Development effort under program element number 62766N, project number ZD62. Current sponsorship in FY 81 is through the NAVAIR Fiber Optic Block Program under program element number 62762N, project number WF625.

The following technical personnel at NOSC were major contributors to the development: SJ Cowen, JH Daughtry, M Kono, JT Redfern, JD Stachiw, RW Urich, and C Young.

Released by  
IP Lemaire  
Advanced Systems Division

Under authority of  
HR Talkington  
Ocean Technology Department

~~UNCLASSIFIED~~

SECURITY CLASSIFICATION OF THIS PAGE (When Data Entered)

**UNCLASSIFIED**

**SECURITY CLASSIFICATION OF THIS PAGE (When Data Entered)**

**20. ABSTRACT (Continued)**

excess of 10 000 psi pressure differential as well as tolerating a wide temperature range. The design lends itself to hermetic construction for applications requiring no vapor diffusion over long mission durations. Such devices exhibit excellent potential for satisfying SUBSAFE requirements for manned submarine applications.

X

A

**UNCLASSIFIED**

**SECURITY CLASSIFICATION OF THIS PAGE(When Data Entered)**

## CONTENTS

	<u>Page</u>
INTRODUCTION . . . . .	1
REALIZATION . . . . .	3
THEORETICAL CONSIDERATIONS . . . . .	6
OPTICAL MEASUREMENTS . . . . .	10
MECHANICAL CONSIDERATIONS . . . . .	15
MECHANICAL TOLERANCES . . . . .	19
CONSTRUCTIONAL REALIZATION . . . . .	22
PRELIMINARY TEST RESULTS . . . . .	25
SUMMARY . . . . .	27
CONCLUSION . . . . .	28
REFERENCES . . . . .	29

## ILLUSTRATIONS

Figure 1. Schematic - Graded Refractive INdex (GRIN) rod lens - combination pressure barrier and imaging device.	3
Figure 2. Prototype fiber optic penetrator.	5
Figure 3. Ray trace of SELFOC lens immersed in a fluid medium.	6
Figure 4. Parametric plots for the case of symmetrical lens-to-connector spacing conditions.	8
Figure 5. Chromatic pitch dependence vs wavelength for NSG type SLS/2mm SELFOC rod lens.	9
Figure 6. Attenuation vs position characterization test apparatus.	10
Figure 7. Butt-coupled fiber configuration.	12
Figure 8. Transverse displacement loss of butt-coupled optical fibers.	12
Figure 9. Experimental configuration employed to evaluate the insertion loss of SELFOC lens.	14
Figure 10. Transverse displacement loss of optical fibers imaged by 0.499 pitch SELFOC lens.	14

ILLUSTRATIONS (Cont)

	<u>Page</u>
Figure 11. Longitudinal displacement loss of optical fibers imaged by 0.499 pitch SELFOC lens.	15
Figure 12. Plate covering a 1-inch diameter mounting hole, modeling considerations.	16
Figure 13. Plate deflection model, simply-supported edges.	17
Figure 14. Results of plate deflection modeling for an applied pressure of 10,000 psi.	17
Figure 15. Alignment mechanism, Amphenol Type 906® fiber optic connector.	19
Figure 16. Fiber optic penetrator assembly.	23
Figure 17. Prototype penetrator prior to final assembly.	24
Figure 18. Assembled penetrator.	24
Figure 19. Detail of alignment plate adjustment for maximum optical signal throughput.	25
Figure 20. Detail showing Delrin® alignment sleeve normally employed to align Amphenol Type 906 fiber optic connectors.	26
Figure 21. Pressure tolerance test configuration.	27

## INTRODUCTION

This program was undertaken as an effort aimed toward developing generic concepts and prototype designs for a high pressure undersea bulkhead penetrator for use in conjunction with fiber optic cables employed in the deep ocean environment. Watertight optical interfacing devices will be required in order to realize practical underwater systems employing fiber optic cables for command, control, and communications. Optical penetrators may also be required in systems utilizing optical fibers as sensors. Because the penetrator provides the means by which the optical signals carried by the fiber are transferred between the high hydrostatic pressure environment of the cable and the low pressure environment of the electronics package or manned portion of an underwater system, it is a key component required in practically all proposed fiber optic applications under the ocean.

A viable and flexible fiber optic penetrator design would incorporate many features which have historically evolved in the case of presently available electrical penetrators. Unless these proven features are supported, undesirable system impacts might occur which would negate many of the advantages inherent with fiber optic cables compared to their coaxial cable counterparts.

\* The penetrator design should exhibit low optical throughput attenuation. Insertion loss characteristics should be comparable to, and at least as repeatable as, the better optical fiber connectors presently available in the marketplace. The optical characteristics should be maintained over the entire spectral region utilized for communications.

\* The penetrator design should lend itself to efficient certification procedures. It should be possible to test and certify the pressure-integrity function of the device at the time of manufacture - prior to integration with the cable and optoelectronics. Ideally, the pressure barrier subcomponent should be standardized and type certified and should lend itself to integration with any type of optical fiber or connector when incorporated into its final penetrator configuration.

\* The penetrator-to-cable interface should be fully demountable from both the high and low pressure sides of the bulkhead. Ideally, the high pressure side should be capable of underwater make/break operation, a valuable asset for some important system applications. Full demountability obviates the requirement for treating the penetrator, the optoelectronics assembly and the cable as a single unit. It allows separation for the purpose of repair, exchange, transport, and storage of the individual subsystems over the life and mission profile of the system.

\* The design should be compatible with a wide variety of optical fiber and optical connector types. This reduces the certification burden as well as minimizing inventory requirements. One penetrator type should be capable of operation with a wide variety of optical fiber and connector styles via a standardized, type-accepted body.

\* The design should be inherently straightforward to manufacture in a repeatable fashion while maintaining reasonable manufacturing tolerances. It should not be so complex that reliability and cost-effectiveness are compromised.

\* The design should be rugged and robust, permitting operation over a wide range of temperature and pressure conditions. It should be resistant to damage by vibration and explosive shock. Overall system performance must not be compromised in any way due to limitations of the fiber optic penetrator.

\* The design should lend itself to hermetic realizations for applications requiring sustained exposure to high hydrostatic pressures. For reliability, the design should resist vapor intrusion. Glass-to-metal or glass-to-ceramic seals should be incorporable so as to form a hermetic vapor barrier without requiring a major redesign or recertification effort.

Historically, epoxy-filled hypodermic needles, epoxy pottings, and elastomeric squeeze bushings (references 1 & 2) have been employed when it is required to transfer light from an optical fiber across a pressure gradient. These techniques all realize their light transfer function by means of physically sealing to the external cable sheath or to the optical fiber itself. Such approaches fail to satisfy all or most of the criteria describing a viable penetrator realization as stated above. While sometimes serving as adequate solutions when applied to test and evaluation of developmental fiber optic components, reliance upon these techniques is unrealistic and would result in undesirable engineering and operational compromises if applied to Navy system applications.

This report discusses a prototype penetrator design developed at the Naval Ocean Systems Center, potentially satisfying all of the above requirements. Testing is currently underway to more fully characterize device performance as a function of applied environmental stress. The results of the testing will be reported at a future date. The analysis and prototyping

---

1. Redfern, J., Taylor, H., Eastley, R., Albares, D., "Fiber Optic Towed Array," NUC TP 414, October 1974, p 22 - 24
2. Ockert, D., "An Underwater Penetrator Development in Fiber Optics," Oceanic Engineering Report Number 79-23, Westinghouse Oceanic Division, Contract IR and D:78615, 30 April 1979

performed in the development of this particular design has proved to be an important first step toward realizing workable undersea penetrators for future Navy applications employing optical fiber cables.

#### REALIZATION

The penetrator realization reported here is based upon the concept disclosed in reference 3. This approach utilized a GRIN rod lens of one half pitch length as a combination pressure barrier and imaging device, schematically depicted in figure 1. Because this concept, as reported, predicated the availability of low-loss single optical fiber cables (circ 1973) it was predicated for use in conjunction with optical fiber bundle technology. If this realization is to be a viable approach capable of performing compatibly with modern, low-loss, single optical fiber technology, several key questions must be answered.

### OPTICAL FIBER HIGH PRESSURE PENETRATOR DESIGN "A"

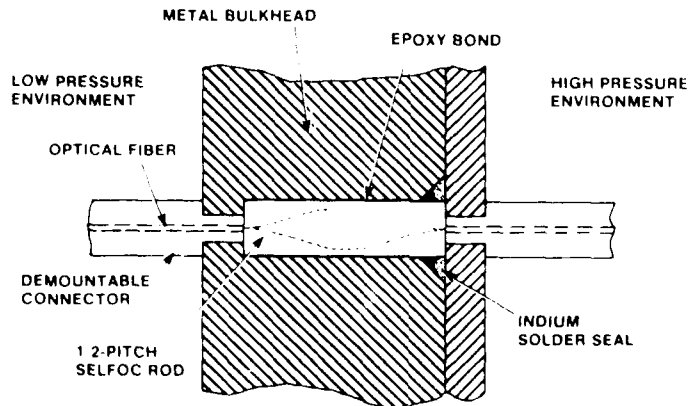


Figure 1. Schematic - Graded Refractive Index (GRIN) rod lens = combination pressure barrier and imaging device.

\* Do contemporary GRIN lenses (circ 1980) whose optical properties have been refined compared to their 1970 vintage forerunners, exhibit adequate focusing acuity to permit

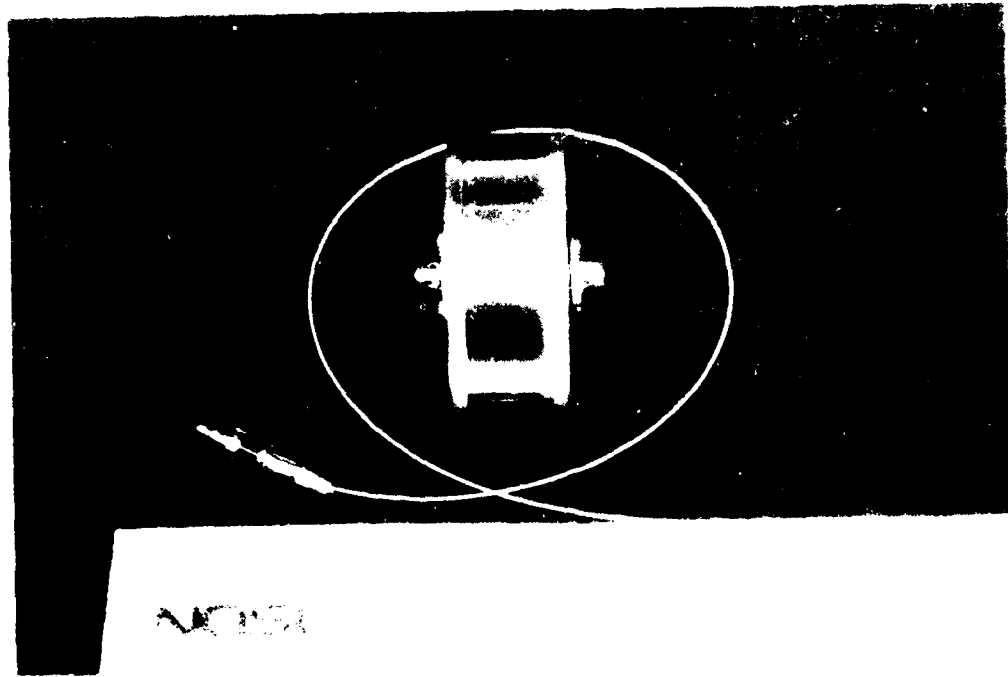
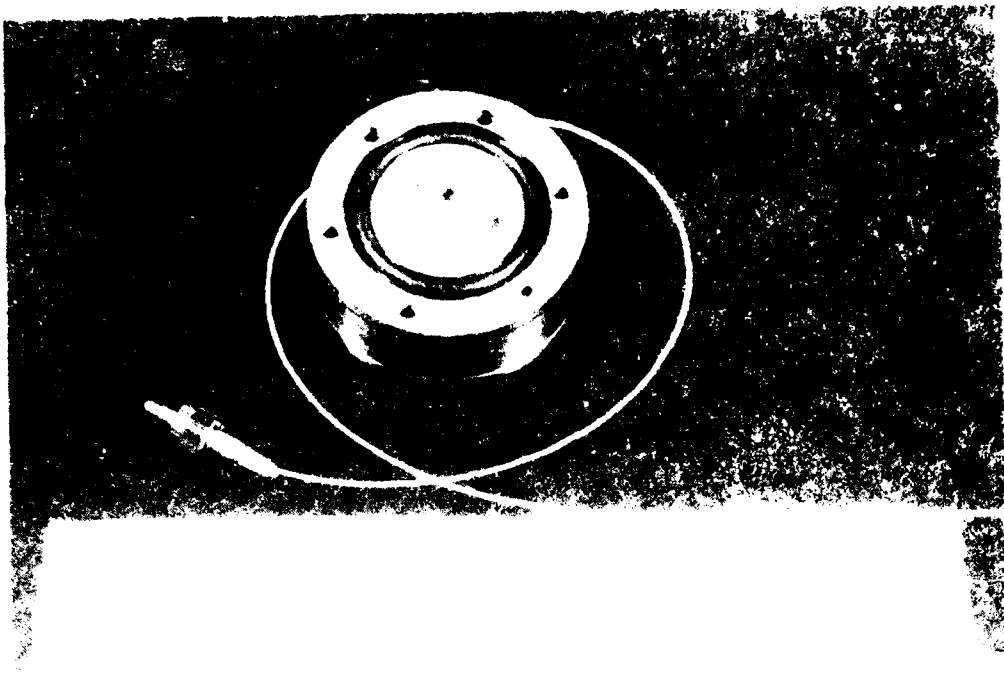
3. Redfern, J. "High-Pressure Optical Bulkhead Penetrator," United States Patent 3,825,320, filed 2 March 1973, granted 23 July 1974

imaging the 50 micron core of a typical low-loss optical fiber onto a conjugate receiving fiber without the loss of an appreciable fraction of the light energy? What are the prospects for such devices to be used in conjunction with single mode optical fibers which will be employed with some fiber optic communications and sensor systems in the future?

\* Can such rod lenses be mounted in a sufficiently stable manner to permit reliable operation over a wide range of pressure and temperature conditions? This consideration is important because any rod movement with respect to the connectors will result in the defocusing or translation of the image with a resulting increase in insertion loss.

\* Is it practical to fabricate a heavy penetrator body capable of withstanding in excess of 10,000 psi pressure differential to the required mechanical tolerances necessary to mate pairs of single fiber connectors in a repeatable manner? If not, what combination of machining and alignment features should be employed to enhance fabrication techniques?

As a result of the research performed in this 6.2 development program we are reasonably confident that practical, high performance fiber optic pressure penetrators, utilizing the concept presented here, are entirely realizable. Practical production devices are possible to manufacture if suitable fabrication techniques are employed. Prototype demountable penetrator units developed at NOSC, utilizing the one-half pitch GRIN lens window concept, combined with refinements relating to positional rod location and connector transverse alignment, exhibit approximately 1-1.5 dB optical insertion loss, making them optically comparable to many of the better fiber optic connectors themselves. Intrinsic insertion loss of the GRIN lens is on the order of 0.3 dB; this permits a very low level of insertion loss to be realized in nondemountable designs. Prototype penetrators have been tested to hydrostatic pressures in excess of 10,000 psi (corresponding to maximum depths commensurate with over 95% of the ocean floor) without failure. No degradation in optical performance was observed after high pressure "soaks" lasting several days; this indicated that inconsequential positional creep in rod position was taking place due to long-term applied stress. Temperature cycling over a range from -40°C to +100°C caused no glass spalling due to mismatch of temperature coefficients between glass and metal. A photograph of a prototype fiber optic penetrator is shown in figures 2a and 2b.



NOTE:

## THEORETICAL CONSIDERATIONS

The GRIN rod lens chosen for consideration was the SELFOC® Type SLS/2 mm manufactured by the Nippon Sheet Glass of Japan and distributed by the Nippon Sheet Glass Company, USA. This unit exhibits the following characteristics:

Numerical Aperture (NA)	0.30
On-axis Refractive Index ( $n_s$ )	1.545
Radial Grading Constant (A)	0.0361
Nominal Diameter	2.0 mm
Nominal Pitch Length	32.8 mm
Cost in 1980, Unit Quantities	\$40

The type SLS GRIN lens appears to be the best choice among SELFOC products in that it exhibits adequate numerical aperture to collect nearly all the light emitted from a low-loss graded index optical fiber (whose NA typically ranges from 0.14 to 0.28). Relatively moderate chromatic pitch dependence is inherent in the Type SLS compared to larger NA devices such as the Type SLW. This is very important in the case of wavelength duplexed communications link applications. Two mm corresponds to the largest standard diameter presently available in the SELFOC line although larger diameter lenses have been fabricated and are currently being transitioned into production. Larger diameter lenses minimize the mechanical interfacing mismatch of lens to connector, facilitating fabrication. Likewise, ultra-high resolution SELFOC lenses have been developed which permit imaging of single mode optical fibers with low loss. The device employed to construct the penetrators reported here is a standard item currently being mass-produced in Japan - mass production keeps reproducibility high and cost low.

Referring to figure 3, equations (1) and (2) describe the imaging rules of a SELFOC lens, modified for the case where the device is immersed in a matching fluid medium.

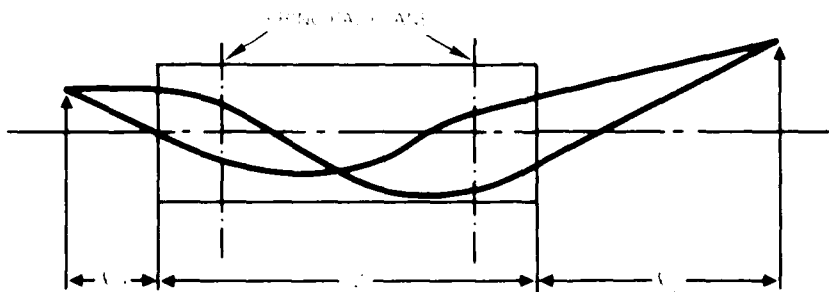


Figure 3. Ray trace of SELFOC lens immersed in a fluid medium.

$$l_1 = \frac{n}{n_s\sqrt{A}} \frac{n_s l_2 \sqrt{A} \cos \sqrt{A}Z + n \sin \sqrt{A}Z}{n_s l_2 \sqrt{A} \sin \sqrt{A}Z - n \cos \sqrt{A}Z} \quad (1)$$

$$P = \frac{\sqrt{A}Z}{2\pi} \quad (2)$$

where:  $l_1, l_2$  = Image plane positions

Z = Length of SELFOC lens

A = SELFOC lens radial grading constant

$n_s$  = Refractive index of the SELFOC lens on the optical axis

n = Refractive index of the medium surrounding the SELFOC lens

P = SELFOC lens fractional pitch length

If the SELFOC lens is chosen to be exactly one-half pitch length, an object in contact with one face creates an inverted, real image of itself (at unity magnification) on the opposite face. This would be undesirable in a practical penetrator realization because of the possibility of entrapping grit between the lens face and the connector end, scratching both the lens and the fiber held by the connector. A small setback between lens face and connector, implying that imaging should occur slightly outside of the SELFOC lens, is desirable. As determined by equations 1 and 2, this requires that the lens length be slightly less than one-half pitch.

Equations (1) and (2) are plotted in figure 4 for the case of symmetrical lens-to-connector spacing conditions where the rod lens is immersed in an oil medium having a refractive index of 1.50.

It is noted that an optimum locus of conjugate spacing ( $L = l_1 = l_2$ ) occurs which is relatively linear over the dimensions of interest, 25 - 100 micrometers (0.001 - 0.004 inch). In this region, the required pitch length can be quickly determined by employing a linear regression approximation as expressed by equation (3).

$$L = 11210 - 22419P \quad (3)$$

where:

L is in micrometers, and

P is the SELFOC lens fractional pitch length

For example, in order to achieve a 38.1 micrometer clearance dimension between lens face and connector (0.0015 inch) a lens fractional pitch length of 0.4983 inch is dictated.

Because the refractive index of all transparent materials is a function of wavelength and because SELFOC lenses are composed of a glass composite (thallium-doped borosilicate in the case of the Type SLS), the pitch length of

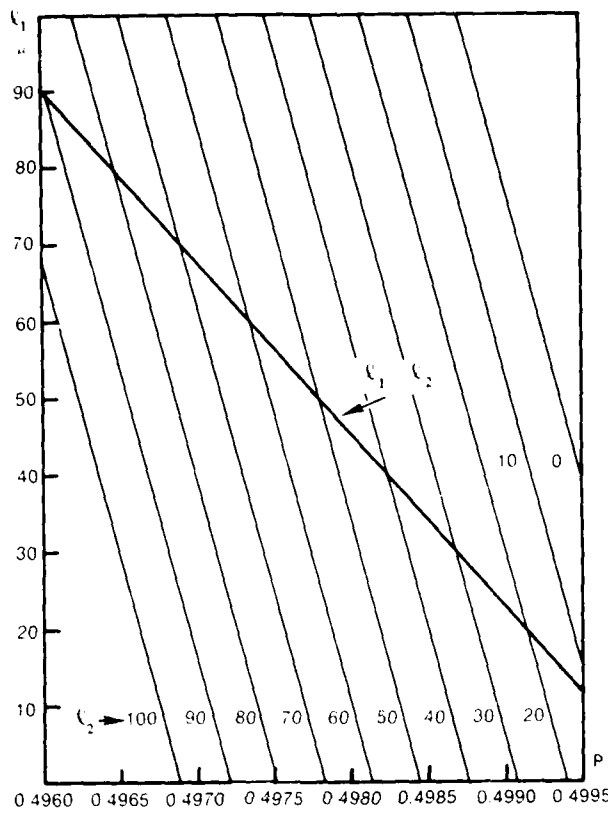


Figure 4. Parametric plots for the case of symmetrical lens-to-connector spacing conditions.

a given lens is a function of wavelength. This implies that the clearance dimensions calculated above depend upon the wavelength of light transmitted through the lens. In the case of wavelength multiplexed or duplexed transmission schemes, the lens face/connector standoff dimension can only be "correct" at 1 wavelength. It is necessary in such cases to predict the performance degradation expected insofar as insertion loss is concerned.

The pitch length of a SELFOC lens is given by equation (4) and wavelength dependence of the glass composing the Type SLS lens by equations (5a and 5b).

$$Z = \sqrt{2\pi PR} \sqrt{\frac{n_o(\lambda)}{\Delta n(\lambda)}} \quad (4)$$

$$n_o = 1.5345 + 7.40 \times 10^5 / \lambda^2 \quad (5a)$$

$$n_R = 1.5076 + 5.00 \times 10^5 / \lambda^2 \quad (5b)$$

where:

R = Radius of SELFOC lens

$\lambda$  = Optical wavelength in  $\text{\AA}$

$$\Delta n = n_o(\lambda) - n_r(\lambda)$$

Plotting  $dP/P$  as a function of wavelength, figure 5 is obtained. The percentage change in pitch length is normalized to a wavelength separation of 1 micron.

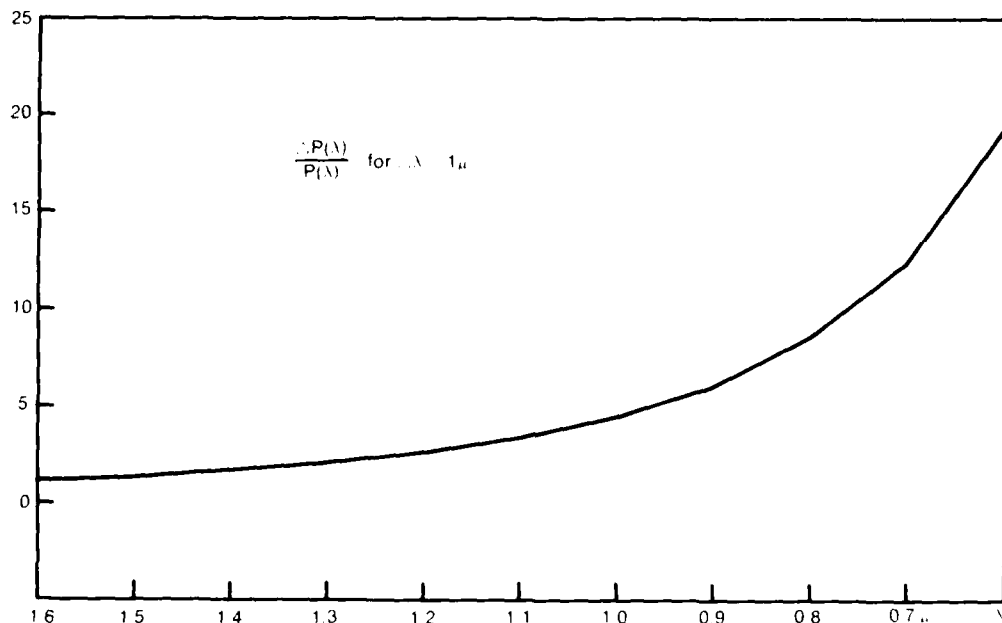


Figure 5. Chromatic pitch dependence vs wavelength for NSG type SLS/2mm SELFOC rod lens.

It is observed that the change in effective pitch length as a function of wavelength is substantial at short wavelengths (ie, the visible portion of the spectrum) but much less pronounced in the near infrared. For example, in the case where the two wavelengths are 0.83 micron and 1.06 microns, as in a typical wavelength multiplexed communications link, a SELFOC rod exhibiting 0.499 pitch characteristics at the short wavelength has an effective pitch length of only 0.491 at the long wavelength. This result will be utilized later in this report to predict the increase in insertion loss which would be exhibited by a penetrator employed under such conditions. Because the trend in high performance fiber optic systems is toward longer wavelengths where optical fiber transmission characteristics are optimized, the example considered above represents a worst-case situation. For example: if the two wavelengths are changed to 1.27 microns and 1.55 microns (corresponding to the

high optical performance spectral windows observed in modern optical fibers), the effective pitch lengths become 0.498 at the short wavelength and 0.496 at the long wavelength. Put another way, the SELFOC rod characteristics appear more nearly achromatic as the wavelengths are shifted farther into the infrared. This is fortunate in that it simultaneously optimizes the data transmission characteristics of the optical fiber as well.

#### OPTICAL MEASUREMENTS

It is desirable to accurately characterize the optical insertion loss encountered when employing the SELFOC rod lens as a fiber imaging element in an undersea penetrator. This section documents optical measurements performed upon a typical unit. The results help to confirm the validity of the penetrator realization and give an indication of the mechanical tolerances necessary to achieve acceptable optical performance.

The optical attenuation apparatus used to characterize the lenses is depicted in figure 6.

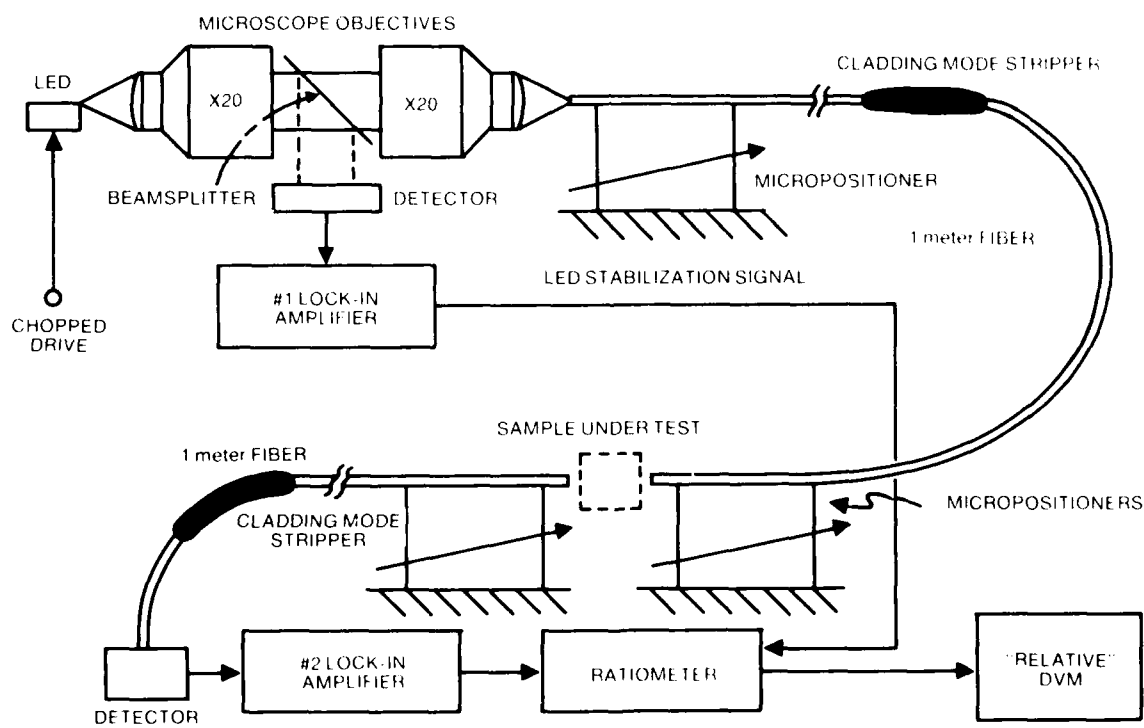


Figure 6. Attenuation vs position characterization test apparatus.

Measurement uncertainty in the instrumentation was due primarily to thermally-induced drift in the micropositioner assemblies; the long-term stability of the setup was approximately 0.03 dB/hour. The data presented here are therefore meaningful to a few hundredths of 1 dB insofar as precision is concerned. Micropositioner calibration permitted a mechanical resolution of approximately 5 micrometers (0.0002 inch), hence, the accuracy of the positional measurements is of this order.

A number of parameters were held constant throughout the entire series of measurements:

Wavelength	0.83 micron
Fiber Type	ITT Type T-212 GI MCVD
Index Matching Fluid	Glycerin ( $n = 1.4746$ )
SEFOC	NSG Type SLS/2 mm
	0.499 pitch at 0.83
	micron wavelength

Several SELFOC lenses from the same production run were evaluated. Because the results agreed within a few percentage points between units, the measurements obtained with a "typical" SELFOC lens are presented.

The optical fiber employed in the test is typical of modern, low-loss (3 dB/km) graded index telecommunication fibers and conforms dimensionally to the 50/125 micron international core/cladding standard dimensions. The fiber has an advertised short length numerical aperture (NA) of 0.22 which is relevant because 1 meter lengths were employed in the test setup in order to give insertion loss performance approaching worst case. Very long fiber lengths would exhibit somewhat reduced effective NAs (the modal equilibrium condition is approached) which would result in better focusing by the rod lens, hence, lower insertion loss.

As a baseline measurement it is informative to consider optical insertion loss as a function of lateral alignment mismatch for two butt-coupled, graded index optical fibers. The fiber faces were prepared by the diamond scribing and fracture technique (reference 4) and were quite flat and uniform. Glycerin was employed as the refractive index matching fluid between the cleaved fiber faces serving to minimize loss due to Fresnel reflection. Its optical properties closely approximate those of mineral oil which is used in the final penetrator design. The configuration is depicted in figure 7.

When the optical fibers were "perfectly" aligned, the light throughput was defined to be unity (0 dB). The insertion loss was, therefore, nonzero for any mechanical misalignment from the "perfect" location. Insertion loss as a function of transverse displacement is shown in figure 8 for the case of two, butt-coupled fibers.

---

4. Gloge, D, Smith, PW, Bisbee, DL, Chinnock, FL, "Optical Fiber End Preparation for Low-Loss Splices," Bell Syst Tech J.

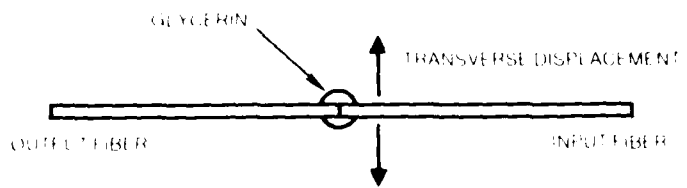


Figure 7. Butt-coupled fiber configuration.

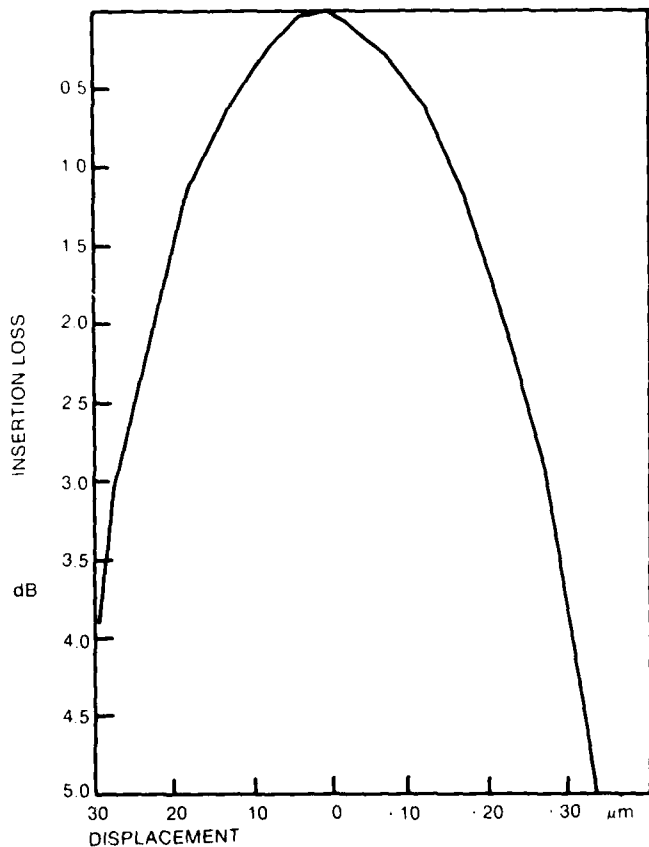


Figure 8. Transverse displacement loss of butt-coupled optical fibers.

Noting that 25.4 micrometers = 0.0010 inch = 1 mil, it can be seen that a lateral misalignment of 11 micrometers (0.43 mil) is sufficient to introduce a light coupling loss of 0.5 dB between the two fibers. A displacement of 19.5 micrometers (0.77 mil) causes a 1.5 dB insertion loss. An insertion loss of 3 dB corresponds to a lateral misalignment of 27.5 micrometers (1.07 mils); in

this case only one half the transmitted power is coupled from one fiber to the other.

The problem faced by designers of commercial fiber optic connectors for 50 micrometer core fibers is quite apparent; that of guaranteeing consistent alignment accuracy for a low-cost, mass produced component.

The penetrator realization developed at NOSC utilizes a nominally one-half (0.499) pitch SELFOC lens as an optical relay element. The experimental configuration employed to evaluate the insertion loss of the SELFOC lens for such applications is depicted in figure 9.

The insertion loss is plotted in figure 10 as a function of fiber lateral displacement over a range of symmetrical fiber to lens face setback clearances.

It was observed that the insertion loss was minimized for setbacks on the order of 0-25 micrometers, as would be predicted by equation (3) for a SELFOC lens of 0.499 pitch length ( $l_1 = l_2 = 22$  micrometers). Insertion loss increases rapidly for setbacks exceeding approximately 40 micrometers. Near the optimum setback distance, transverse alignment tolerances are comparable to those observed with butt-coupled fibers, implying that the image of the fiber core is distinct. As the setback distance increases, causing the image to defocus, the tolerances relax somewhat; the larger, blurred image is easier to maintain aligned with the receiving fiber. This indicates a tradeoff between insertion loss and criticality of alignment. Measured insertion loss as a function of setback distance, assuming perfect transverse alignment, is given by figure 11, for the case of a 0.499 pitch lens immersed in glycerin.

This experiment demonstrates for the case of "perfect" fiber alignment, that the insertion loss of a typical SELFOC relay lens is nominally 0.3 dB under the conditions evaluated. In order to maintain less than 1.0 dB of total insertion loss in a demountable pressure penetrator, the transverse, peak fiber alignment error must be less than 11 micrometers. Longitudinal tolerances of less than 38 micrometers must be maintained. In the case where a total insertion loss of 3 dB is tolerable, peak tolerances must be less than 22 micrometers and 100 micrometers, respectively.

Because the chromatic dependence of the lens introduces an effect similar to that of altering pitch length as a function of wavelength, the results of figures 10 and 11 can be employed to estimate the increase in insertion loss due to chromatic aberration. In the case of a penetrator optimized for operation at 0.83 micron, the effect of introducing 1.06 micron light is the same as reducing the pitch length of the rod lens from 0.498 to 0.491 but not reoptimizing end clearances. This would result in approximately 3-4 dB of additional insertion loss. The magnitude of this effect can be reduced by optimizing the penetrator at a wavelength intermediate to the two wavelengths specified, using, perhaps, a SELFOC lens pitch length of 0.495. This tradeoff approach is clearly system dependent because the transmission link may operate with much greater margin at the longer wavelength (this is usually the case), hence, the link may be able to afford greater insertion loss at the penetrator. Fortunately, this effect is much less severe at the long wavelengths presently contemplated for long-haul, undersea system applications. For example, if the previous wavelengths are changed to 1.27 and 1.55 microns, the

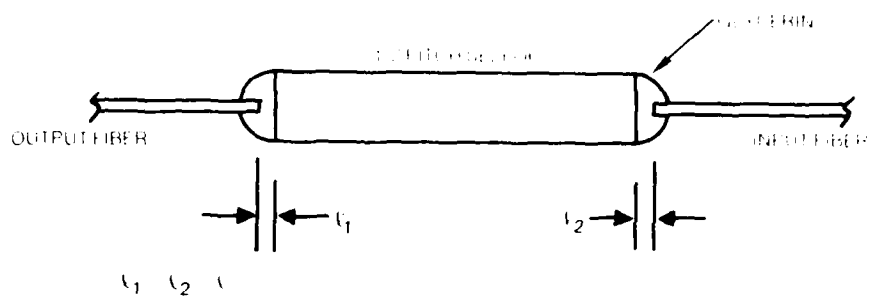


Figure 9. Experimental configuration employed to evaluate the insertion loss of SELFOC lens.

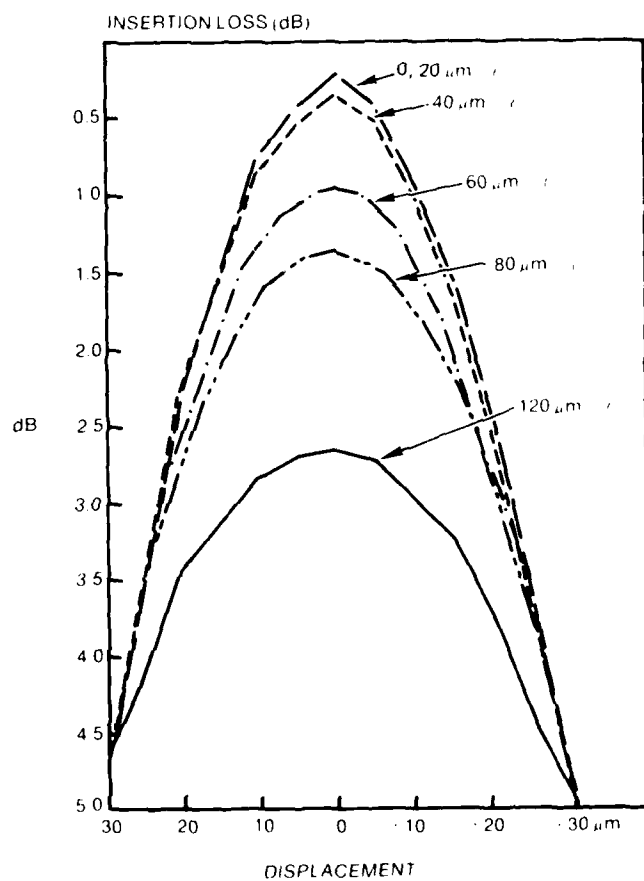


Figure 10. Transverse displacement loss of optical fibers imaged by 0.499 pitch SELFOC lens.

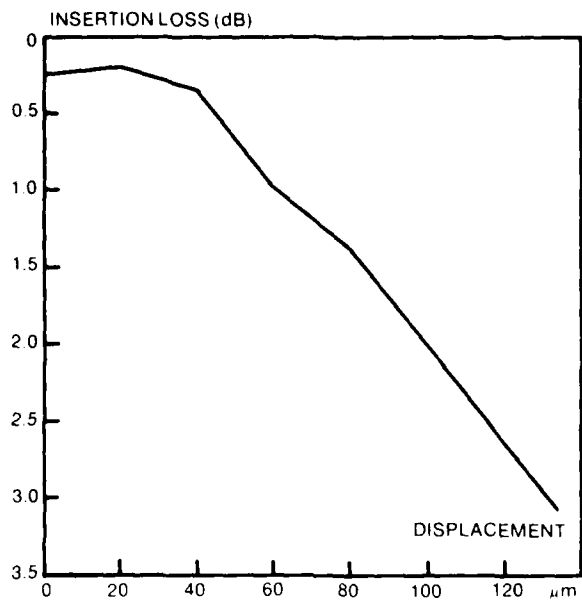


Figure 11. Longitudinal displacement loss of optical fibers imaged by 0.499 pitch SELFOC lens.

increased insertion loss at the longer wavelength is approximately 0.8 dB if the penetrator is optimized at the shorter wavelength. Optimization of the penetrator at an intermediate wavelength would result in even smaller chromatic effects.

#### MECHANICAL CONSIDERATIONS

In order to predict environmental performance of the penetrator design it is necessary to determine the mechanical effects due to externally applied stimuli: differential pressure (glass stress, epoxy shear) and temperature cycling (glass compressive stress).

Glass stress was modeled as a function of pressure by considering a circular steel disk with a centrally located 0.080 inch diameter hole to approximate the condition encountered when a SELFOC rod is bonded into a metal bulkhead. This assumption implies that the glass, which would fill the hole in the actual device, exerts no restoring force upon the metal surrounding it. This corresponds to a worst-case assumption insofar as plate deflection is concerned. The plate was assumed to cover a 1-inch diameter mounting hole as depicted in figure 12.

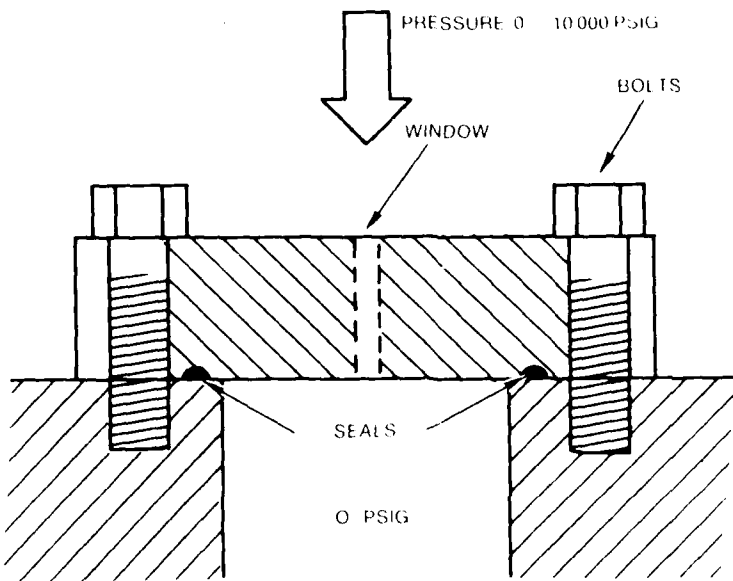


Figure 12. Plate covering a 1-inch diameter mounting hole, modeling considerations.

The plate deflection was calculated as a function of applied pressure differential for the extreme cases of fixed and simply supported edges (reference 5). The latter was found to exhibit greater deflection as a function of applied pressure and is reported here because it gives more conservative results. Such a case is shown in figure 13.

Results of the modeling are given in figure 14 for an applied pressure of 10,000 psi. Plate displacement due to flexure, hole radius contraction (at the high pressure surface), and tensile load on the steel plate are plotted vs plate/window thickness.

The failure mode of the glass was hypothesized to be spalling of the edges of the high pressure face of the SELFOC lens due to the uneven compressive forces acting upon the window as a result of plate flexure under applied pressure. This hypothesis was verified experimentally utilizing a 0.250 inch thick glass window mounted in a type 1704 stainless steel bulkhead using a hard solder sweat. Failure due to spalling of the edges of the window was first observed when the applied pressure exceeded 5000 psi, corresponding to a calculated plate deflection of 0.001 inch, a change in hole radius of 0.0005 inch at the high pressure surface, and a stress level in the steel of 90,000 psi. No leakage occurred at a pressure of 11,500 psi (the limit of our test equipment), even though the high pressure side of the window was badly spalled and glass fractures in planes parallel to the bulkhead had formed. The low pressure side of the window remained intact. Because the bulkhead containing the SELFOC rod in the penetrator design reported here is approximately 0.65 inch thick, window failure at a pressure of 50,000 psi can be

5. Roark, RJ, Formulas for Stress and Strain, McGraw-Hill, NY, 1965.

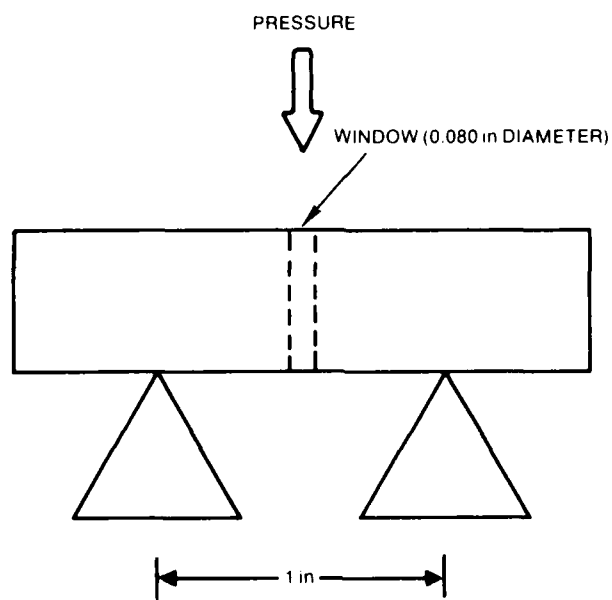


Figure 13. Plate deflection model,  
simply-supported edges.

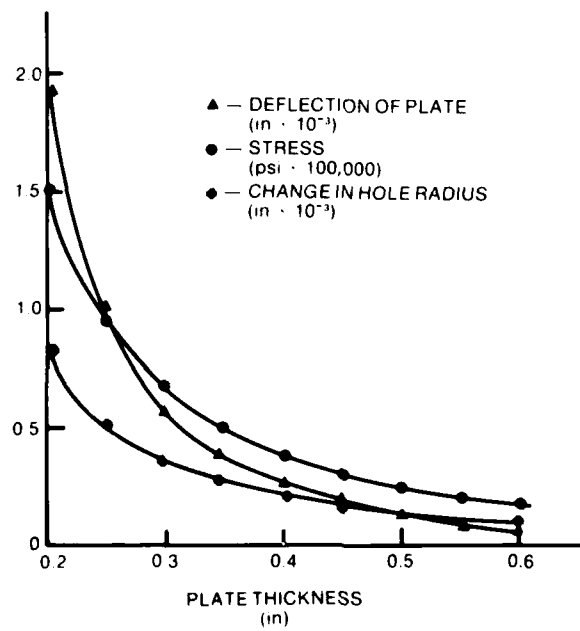


Figure 14. Results of plate deflection  
modeling for an applied pressure of  
10,000 psi.

inferred from figure 14 due to glass spalling. Plate deflection corresponds to less than 0.0001 inch at a working pressure of 10,000 psi. Stress upon the steel is only 20,000 psi; this allows for the employment of a low-strength metal alloy selected for free cutting properties and corrosion resistance criteria instead of tensile strength. A safety factor of approximately five at an applied pressure of 10,000 psi is inferred for glass breakage.

The shear force acting upon the epoxy employed to bond the SELFOC rod into the metal bulkhead was calculated using equation 6, derived from geometrical considerations.

$$S = \frac{1}{4} P (d/l) \quad (6)$$

where:

S = Shear force

P = Pressure differential

d = SELFOC lens diameter

l = SELFOC lens length

The aspect ratio (d/l) of a type SLS SELFOC lens is 0.122, independent of rod diameter. The epoxy employed is Epotek™ Type 301-2 which is specified as having a lap shear strength (aluminum to aluminum) of 2,000 psi. Allowing the epoxy shear strength to be derated to 1,000 psi for the case of glass to steel bonding (probably conservative), the epoxy will shear at an applied pressure level of 33,000 psi, corresponding to a safety factor of at least 3-4 for the epoxy bond.

The thermal stress effect was modeled by a 0.080 inch diameter borosilicate crown glass rod in intimate contact with a 2.0 inch diameter concentric stainless steel annulus. Because the temperature coefficient of the metal is greater than that of the glass, the metal is expected to squeeze the glass at cold temperatures, placing it under stress. Under these assumptions, the glass is subjected to a radial compressive loading of 1,030 psi when cooled from +20 F to -20 F (reference 6). This is well below the 50,000 psi compressive strength typical of soft glasses. Because the glass and metal are not actually in intimate contact, but have a thin film of epoxy between them (which has an elastic modulus approximately a factor of 30 less than either the glass or the metal), the above calculation is quite conservative. In practice, the epoxy acts as an elastic cushion layer which effectively reduces compressive and tensile loading upon the glass. The penetrator is expected to pass MIL temperature cycling over the range of -55 C to +125 C in storage at 1 atmosphere. Whether the device can maintain satisfactory operational insertion loss under such conditions and remain within optical specifications is currently under determination.

---

6. Gatewood, RC, Thermal Stresses: With Applications to Airplanes, Missiles, Turbines, and Nuclear Reactors, McGraw-Hill, 1957.

## MECHANICAL TOLERANCES

The mechanical tolerances which must be maintained in order to assure satisfactory optical performance for a demountable fiber optic penetrator (or connector) are quite stringent. In order to achieve less than 1.5 dB of total insertion loss due to misalignment and defocusing, it was determined from figures 10 and 11 that the following peak mechanical tolerances in locating the fiber cores must be achieved in production and maintained in the field:

Transverse	less than 15 micrometers, or
Concentricity	less than 15 micrometers, or
Longitudinal	less than 60 micrometers.

These tolerances correspond to those required to mate a pair of 50 micron core, graded index telecommunication fibers in an "optically satisfactory" manner. Each tolerance corresponds to a peak value and assumes that all other mechanical misalignment is negligible. For the purpose of this analysis, peak displacement error values are employed; it is assumed that multiple misalignments add in an RMS manner (average errors accumulate). In practice, the possibility exists for poorer (or better) performance because peak values may add (or subtract) constructively. On the average, however, such events appear to be relatively improbable.

The connector selected to mate with the prototype penetrator is the Type 906™, as manufactured by Amphenol, Incorporated. A drawing indicating the construction of the alignment mechanism of this device is shown in figure 15.

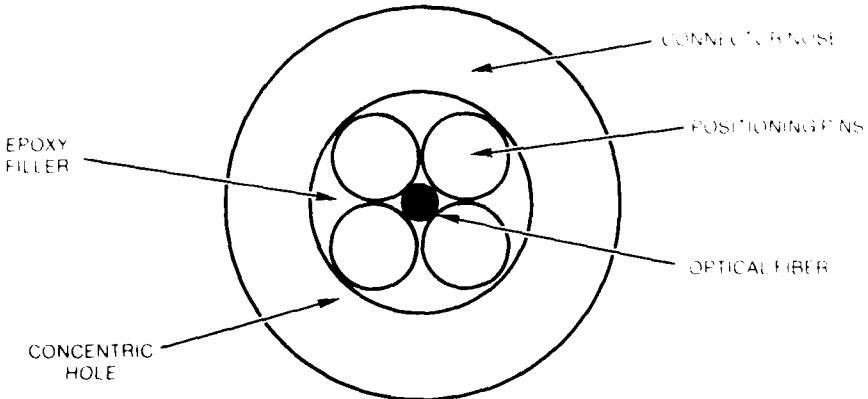


Figure 15. Alignment mechanism, Amphenol Type 906® fiber optic connector.

This connector uses four roller bearings pressed into a relatively large diameter hole bored in a precision-machined plug body to achieve accurate optical fiber core alignment. The optical fiber is inserted through the hole formed between the roller bearings and is epoxied into place and lapped to length. A subsequent polishing operation assures an acceptable optical finish on the face of the fiber. The entire installation procedure, exclusive of the

epoxy curing time, takes about 30 minutes. In normal use, a unit is mated to a second identical connector using a precise, injector molded DELRIN™ sleeve to achieve transverse and longitudinal alignment. Insertion loss less than 1.5 dB (typical) is claimed by the manufacturer. The Type 906 was employed in our application for several reasons:

- It is of stainless steel construction
- Its alignment nose is of small diameter (approximately that of SELFOC lens)
- It is a hermaphroditic design
- It is readily field installable
- It exhibits acceptable insertion loss characteristics
- It is relatively inexpensive
- It is an industry-accepted component.

As more suitable fiber optic connectors become commercially available in the marketplace it is likely that the penetrator design can be altered to accommodate them.

Measurements taken on seven Amphenol Type 906 fiber optic connectors, field installed by the author's group and measured by the NOSC Metrology Laboratory, indicate that the following peak mechanical tolerances are achieved using field installed, production devices:

Transverse	0 (absorbed into fiber diameter)
Concentricity	3 micrometers
Lapped length	5 micrometers

Manufacturer's data from International Telephone and Telegraph Corporation and other optical fiber producers, indicate that the tolerances presently achievable with regard to the optical fibers themselves are on the order of:

Transverse (diameter)	5 micrometers
Core concentricity	5 micrometers
Length	0 (if lapped into a connector)

If tolerances for two connectors are combined and added in an RMS fashion, the total error can be estimated for a mated pair of "perfectly aligned" connectors containing installed fibers:

Transverse	10.9 micrometers
Longitudinal	7.1 micrometers

It is seen that under ideal conditions (an absolutely perfect external alignment mechanism is employed to index the connectors) considerably less than 1.5 dB of total insertion loss should be achievable (misalignment less than 15 micrometers). It is also apparent that it is just barely possible (in theory) to achieve the required 11.0 micron peak tolerance (on the average) necessary to exhibit less than 1 dB insertion loss. The above, of course, postulates an alignment mechanism with no errors of its own. This cannot be the case, hence, tolerances in the penetrator alignment mechanism (particularly transverse errors) will contribute to overall insertion loss and will

begin to dominate if allowed to exceed approximately 10-15 micrometers. Longitudinal tolerance must be held to much less than 60 micrometers if longitudinal misalignment is not to introduce appreciable additional insertion loss. If the longitudinal locating accuracy of the penetrator is better than approximately 5 micrometers, longitudinal errors will be dominated by the length uncertainties of the lapped connectors themselves.

It was determined that the penetrator realization could utilize precision machining operations (turning and lapping) to achieve the required longitudinal alignment accuracy, but that it would be necessary to provide some type of adjustable alignment mechanism which would be permanently locked into position after adjustment to achieve transverse alignment. This is necessary for metal machining considerations and because the optical axis of the SELFOC lens may not correspond exactly to its physical axis. The design presented in this report utilizes a movable stainless steel plate accommodating one connector assembly. This connector assembly is slid upon a film of epoxy resin to achieve accurate transverse alignment with the penetrator body containing the SELFOC lens and the other connector. Upon curing, the epoxy locks the entire assembly into a single unit which is permanently aligned. Currently, investigation is underway in an effort to eliminate the use of epoxy for this function due to possible long-term instability. Electron beam welding is under consideration for joining the alignment plate to the penetrator body in a permanent and stable manner.

Several potential sources of misalignment error exist:

Transverse

Tolerance upon the hole diameter required to accommodate the locating nose of the connector.

Hole ellipticity, contributing to connector wobble.

Longitudinal

Grinding tolerance limitations encountered during fabrication of the penetrator body and alignment plate.

Variations in epoxy film thickness.

From a practical standpoint, the above implies that the hole should be as round as possible and should be no more than 5 micrometers larger than the maximum diameter required to fit the connector nose. This translates to a hole diameter which is controlled to less than 0.0002 inch overall.

Fabrication errors totaling no more than 25 micrometers (0.001 inch) should exist with regard to plate, body machining, and grinding tolerances, plus epoxy film thickness variations. The epoxy must be mixed consistently and applied at a known temperature and clamping pressure so that batch-to-batch variations in film thickness are minimized. Epotek 301-2, catalyzed per the manufacturer's recommendations and applied between 2-inch diameter stainless steel disks with 2.5 pounds of clamping pressure, at 25 C, was empirically determined to form a cured film thickness of 38 micrometers (0.0015 inch).

## CONSTRUCTIONAL REALIZATION

Six prototype penetrator units were constructed during FY80 at NOSC in order to verify the concept presented previously and to provide units for preliminary test and evaluation. An assembly drawing depicting the construction of the units is given in figure 16. Construction is of Type 303 alloy stainless steel.

The penetrator units were constructed in two sections: A penetrator body, which provides the sealing, pressure barrier, and imaging functions, and an alignment plate which permits the required transverse tolerances to be achieved. A pressure equalization hole in the alignment plate allows for oil transfer as the connector is inserted or removed from the penetrator. The SELFOC lenses were bonded into the bulkheads using low viscosity epoxy (Epotek 301-2) which was inserted using a vacuum filling technique to ensure that voids were not formed (reference 7). After approximately 48 hours of curing at 30 C, each completed penetrator body assembly was pressurized to 11,500 psi for approximately 1 hour. (Before-and-after dimensional measurements with a precision dial indicator demonstrated that negligible rod movement due to epoxy creep resulted from this proof test.) In a similar manner, the penetrator body can be certified for pressure and shock integrity prior to integration with other optical components such as connectors and cables. A photograph of a prototype penetrator prior to final assembly is shown in figure 17. An optional indium solder vapor seal can be deposited, bridging glass and metal, if hermeticity is required.

The final assembly process joins the two sections into a complete penetrator assembly. This function is accomplished by X-Y micropositioning the alignment plate (containing an installed Type 906 connectorized fiber) with respect to the penetrator body (containing another such connectorized fiber) in order to maximize the intensity of an optical test signal which is transmitted through the unit while it is installed in the alignment fixture. A 2.5 pound weight serves to press the alignment plate into close proximity with the penetrator body. The plate floats on a thin film of catalyzed epoxy resin, which acts as a lubricant. The epoxy ultimately cures to provide a stable joint which locks the sections together into a unitized penetrator. After the alignment is accomplished, but before the epoxy has set, the assembly is tacked together with several drops of cyanoacrylate instant adhesive (Loctite Type 495®). The cyanoacrylate creates a stable bond in less than 5 minutes which is strong enough to permit handling of the assembled penetrator without allowing plate movement. This permits the aligned but uncured unit to be removed from the alignment fixture for the duration of the epoxy set-up time (approximately 2 days); this frees up the fixture for alignment of other units. A completed penetrator is shown in figure 18.

7. Cowen, SJ, Daughtry, JH, Young, C, Redfern, J, "Undersea High Pressure Bulkhead Penetrator for Use With Fiber Optic Cables", United States Patent, Navy Case No. NOC-86, filed November 1980.

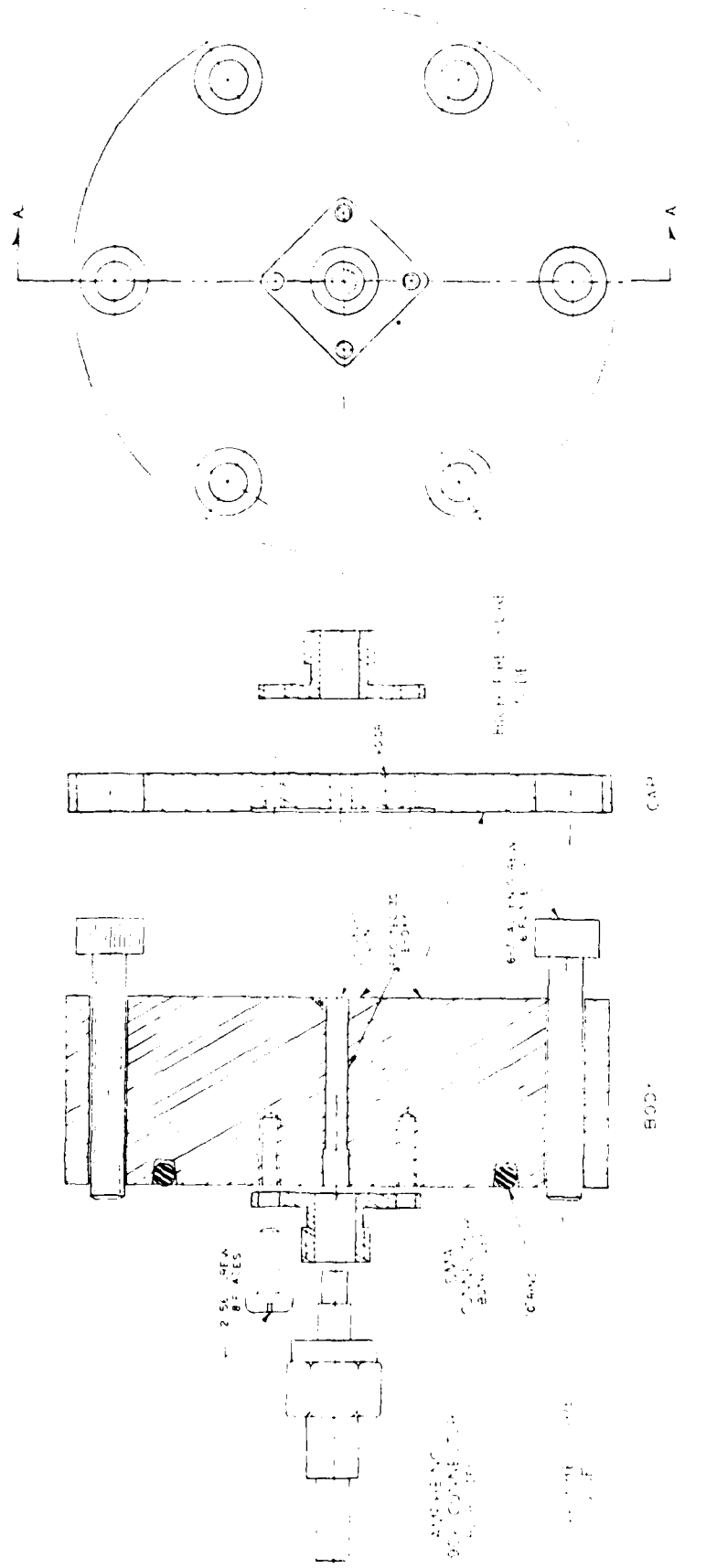
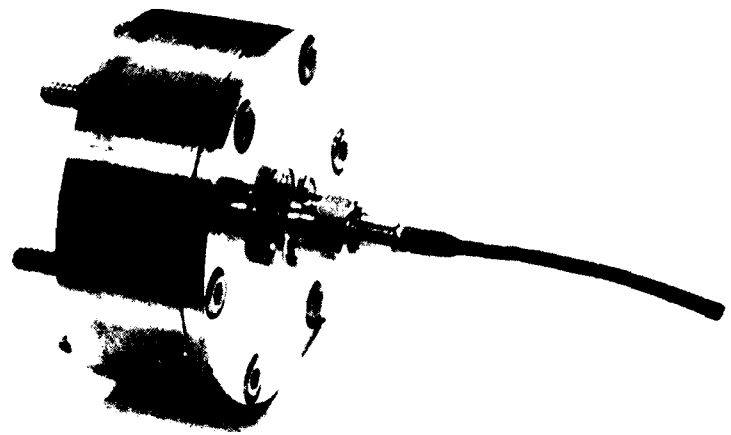


Figure 16. Fiber Optic penetrator assembly.



LRO-2061-7-80B  
Figure 17. Prototype penetrator prior to final assembly.



LRO-2060-7-80B

Figure 18. Assembled penetrator.

#### PRELIMINARY TEST RESULTS

Several tests were performed upon the completed penetrators to determine insertion loss and survivability under applied stress. Extensive characterization of optical performance under stress conditions is currently ongoing in the FYR1 phase of the program and will be reported at a later date.

Insertion loss characterization of the penetrators was performed by inserting a pair of Amphenol Type 906 fiber optic connectors containing 50 micron core, graded index optical fibers into the receptacles (figure 19).

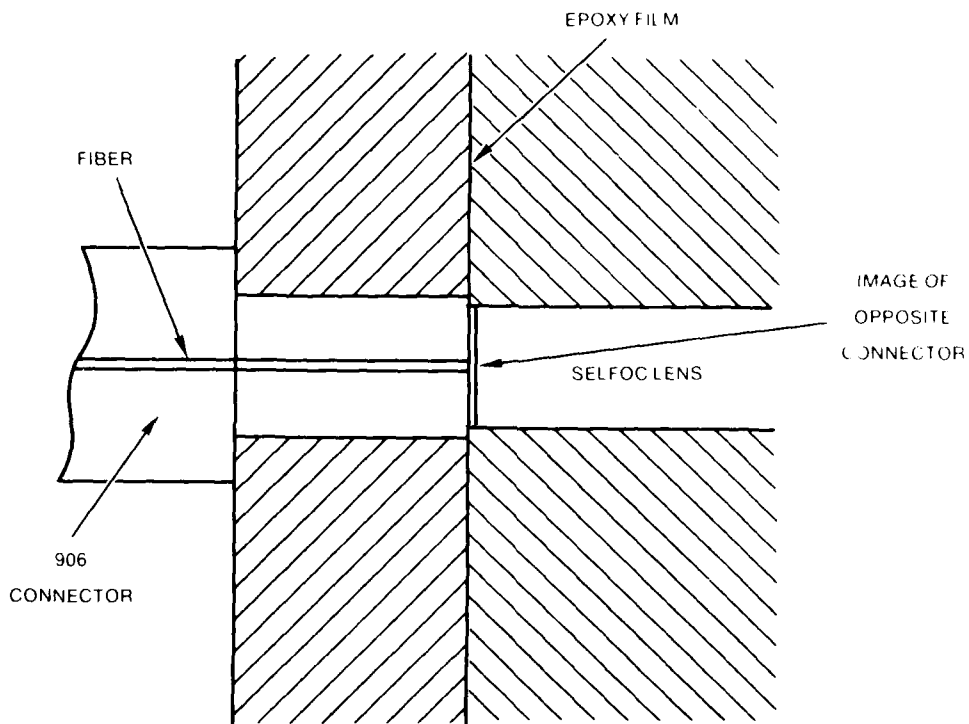


Figure 19. Detail of alignment plate adjustment for maximum optical signal throughput.

Mineral oil (refractive index = 1.50) was used as a combination index matching fluid (serving to minimize Fresnel reflection loss) and lubricant (to prevent metal galling between the connectors and their receptacles). The average insertion loss introduced by a cascade of two connector plugs plus the penetrator assembly was on the order of 1.0-1.5 dB. This is equal to or better than the throughput characteristics exhibited by the connectors when mated in an Amphenol Delrin alignment bushing, the manner in which they are normally employed and as depicted in figure 20. Typically, insertion losses on the order of 1.5-3.0 dB are routinely observed between mated pairs of Amphenol Type 906 connectors used with ITT Type T-212 optical fiber.

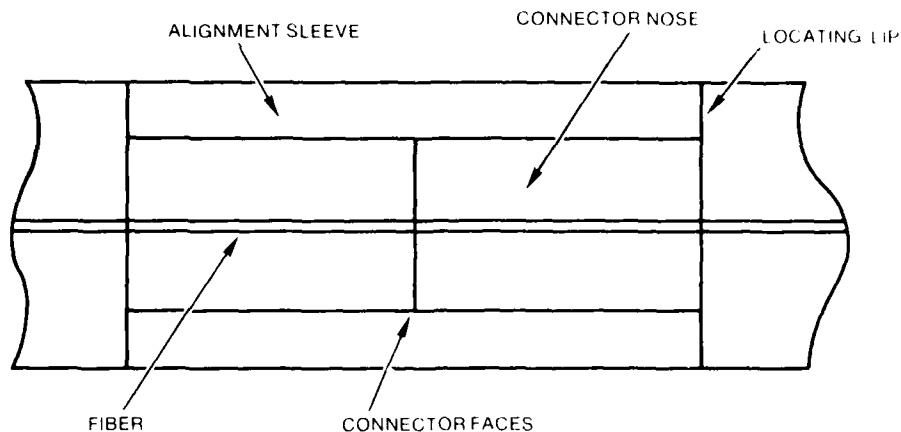


Figure 20. Detail showing Delrin<sup>®</sup> alignment sleeve normally employed to align Amphenol Type 906<sup>®</sup> fiber optic connectors.

Apparently, the alignment accuracy as a result of the adjustable feature of the penetrator design employed here is superior to that exhibited by the factory-supplied, fixed alignment bushing. This increased alignment accuracy is such that it more than compensates for the 0.30 dB insertion loss typical of the SELFOC relay lens which is not present, of course, when the factory-supplied alignment bushing is employed. Considerable variation in throughput level was noted when the connectors were rotated in their respective alignment receptacles, as is the case with the factory-supplied delrin bushing as well. This implies that a major contributor to the alignment error is lack of concentricity of the hole in the connector and of the fiber core within the cladding. Insertion loss as low as 0.5 dB was observed for some of the penetrator units when the connectors were rotated to optimum positions as determined by monitoring throughput power. An even lower insertion loss would be obtainable from a penetrator not requiring the demountability feature.

Ongoing evaluation during FY81 is intended to generate a statistical data base using an ensemble of Type 906 connectors (from various Amphenol production runs) which have been characterized as to insertion loss and an ensemble of penetrator units. This procedure will quantify the worst-case, best-case, and average insertion loss performance figures. These figures will apply to the penetrator design when it is employed with "typical" Amphenol Type 906 connectors. Such data are very valuable in engineering applications where the effect of the penetrator upon the optical performance of a communications link must be predicted when the device is installed in a particular system. Insertion loss as a function of wavelength will also be measured in order to quantify changes in penetrator attenuation due to chromatic aberration in the SELFOC lens.

Survivability to hydrostatic pressure was determined using the apparatus shown in figure 21.

No failure in the penetrator sealing integrity was noted when a pressure of 11,500 psi (the maximum pressure capability of the testing apparatus employed) was applied to the assembly. This pressure corresponds to an ocean depth of

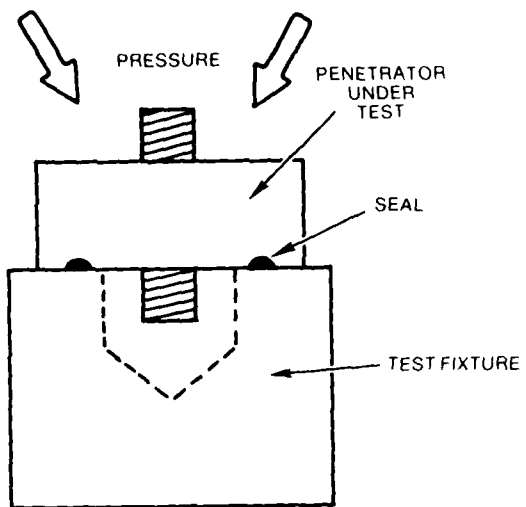


Figure 21. Pressure tolerance test configuration.

23,000 feet. To determine whether epoxy creep and resulting rod movement (which would result under pressure) occurs, the assembly was subjected to 11,500 psi for a period of 3 days at 25 C. Insertion loss measurements performed before and after this soak test indicated that no measurable change in the throughput characteristics occurred. This implied that epoxy creep was small or zero, at least for this combination of time, temperature, and pressure.

Measurements will be taken in order to characterize insertion loss as a function of pressure during FY81. These will determine if any elastic deformation effects are present in the units which would give a pressure-dependent response. The former test, of course, only checks for inelastic deformations.

The penetrators were temperature cycled from +25 C to -40 C to +100 C and back to +25 C to check for glass breakage due to differential stress - none occurred. Throughput characteristics remained the same before and after subjection to temperature extremes. Ongoing characterization will quantify optical throughput characteristics as a function of temperature.

#### SUMMARY

A design for and several prototype models of a high performance, demountable, high pressure penetrator for fiber optic cables have been developed by NOSC. Such devices will be required to realize practical undersea system applications employing optical fiber cables. The approach utilizes the imaging properties of GRIN rod lenses to provide a low insertion loss, high pressure window (which is sealed into the pressure bulkhead). Such an approach overcomes the disadvantages exhibited by previous attempts at realizing fiber optic penetrators, which attempted to seal the fiber itself or the

entire cable jacket into a bulkhead. The GRIN rod approach preserves essentially all of the operational attributes associated with conventional electrical pressure penetrators, making system design using fiber optic cables in the undersea environment more straightforward. Composite connectors containing both fiber optic data transmission elements and electrical power pins are readily realizable using the technique. The realization allows glass-to-metal sealing to be incorporated into the penetrator design for use in conjunction with high-reliability electronic systems.

The prototype penetrators constructed during this program were capable of an optical insertion loss of 0.3 dB in a nondemountable configuration and 1.5 dB when made fully demountable by use of interchangeable optical fiber connectors. In the latter case, the throughput attenuation is dominated by mechanical imperfections in the presently available connectors and optical fibers. The mechanical tolerances required to machine the penetrator alignment receptacles were found to be obtainable using industry-accepted, precision machining techniques. A unique fine adjustment feature incorporated into the realization relaxes the machining requirements associated with the critical connector transverse alignment specifications, making the design readily manufacturable.

Preliminary testing carried out at NOSC has shown the prototype penetrator units capable of withstanding pressures in excess of 10,000 psi with no measurable degradation (this pressure level corresponds to operation with a calculated safety factor of approximately 3 to 4). No damage occurs to the units when cycled between temperatures of -40 C to +100 C. Ongoing testing will characterize optical performance as a function of external stress. Results of the characterization program currently underway during FY81 will be the topic of a follow-on report.

#### CONCLUSION

The design presented here is a promising approach for manufacturing fiber optic undersea penetrators for Navy systems. Desirable operational features traditionally associated with electrical penetrators are readily supported in a fiber optic penetrator when GRIN imaging rods are employed as pressure windows. Prototype devices have been shown to exhibit excellent optical and mechanical performance while simultaneously permitting practical manufacturing techniques to be employed for construction.

REFERENCES

1. Redfern, J., Taylor, R., Eastley, P., Albarez, D., "Fiber Optic Towed Array", NUC TP 414, October 1974, p 22 - 24
2. Ockert, D., "An Underwater Penetrator Development in Fiber Optics", Oceanic Engineering Report Number 79-22, Westinghouse Oceanic Division, Contract IR and D:78615, 30 April 1979
3. Redfern, J., "High-Pressure Optical Bulkhead Penetrator", United States Patent 3,825,320, filed 2 March 1973, granted 23 July 1974
4. Clow, D., Smith PW, Bishop PL, Chinnoch, PH, "Optical Fiber Fme Preparation for Low-Loss Splicing", J. of Opt. Soc. Am., Vol. 69, No. 8, Aug. 1972, p. 1570-1579
5. Roark, RJ, Formulas for Stress and Strain, McGraw-Hill, NY, 1965
6. Gatewood, RC, Thermal Stresses: With Applications to Airplanes, Missiles, Turbines, and Nuclear Reactors, McGraw-Hill, 1957
7. Cowen, SJ, Daughtry, JH, Young, C, Redfern, J., "Undersea High Pressure Bulkhead Penetrator for Use With Fiber Optic Cables", United States Patent, Navy Case No MOSC-86, filed November 1980

